ACS APPLIED MATERIALS & INTERFACES

Research Article

www.acsami.org

Promoting Epithelium Regeneration for Esophageal Tissue Engineering through Basement Membrane Reconstitution

Jingjing Lv, Ling Chen, Yabin Zhu,* Lei Hou, and Yuxin Liu

The Medical School, Ningbo University, Ningbo, China 315211

ABSTRACT: Scaffolds mimicking hierarchical features of native extracellular matrices may facilitate cell growth and anatomical tissue regeneration. In our previous study, esophageal basement membrane (BM) was shown to be composed of interwoven fibers with mean diameter of 66 ± 24 nm (range 28−165 nm) and with abundant pores of unequal sizes. The main extracellular matrix (ECM) contents found in porcine esophageal BM were collagen IV, laminin, entactin, and proteoglycans. In this work, biodegradable polycaprolactone (PCL) and silk fibroin (SF) were spun with electrospinning technology, both individually and in combination, to fabricate fibrous scaffolds with diameters between 64 and 200 nm. The surface morphologies of PCL, PCL/SF, and SF scaffolds were observed under scanning electron microscopy. Their mechanical properties were tested and the cytocompatibility was evaluated in vitro via culture of primary epithelial cells (ECs). The SF or PCL/SF scaffold favorably promoted epithelial cell attachment and proliferation comparing with PCL scaffold. However, mitochondrial activity of epithelial cells was greatly promoted when major BM proteins were coated onto the electrospun scaffold to provide an ECM-like structure. Results from in vivo tests revealed that the electrospun scaffolds coated with BM protein possess good biocompatibility and capability to promote epithelium regeneration.

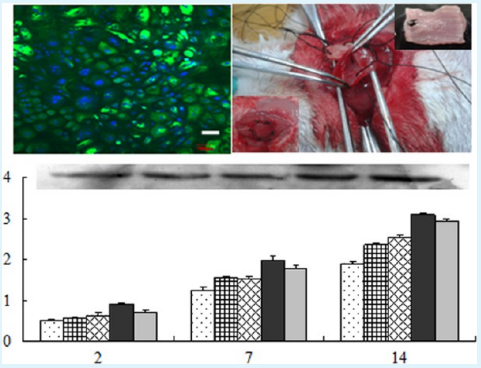

KEYWORDS: *basement membrane, epithelium regeneration, electrospinning, esophageal tissue engineering*

1. INTRODUCTION

Globally, esophageal cancer is the sixth leading cause of cancer-related deaths.[1] Recent reports implied that China accounted for more than 50% of all newly diagnosed esophageal cancers worldwide.[2,3] More than 90% of esophageal cancers originated from the epithelium lining. There are two major subtypes of esophageal cancer; squamous cell carcinoma, which arises from the squamous epithelium, and adenocarcinoma, which arises from the glandular and dysplastic columnar epithelium.[4,5] Because esophagus lacks regenerative capability and there is limited availability of autologous transplants, organ replacement with tissue engineered cell-scaffold constructs is deemed to be a potential strategy for esophageal regeneration in the future.

The esophagus is a muscular tube extending from the pharynx to the stomach. Its main function is to transport food and water from mouth to stomach. The wall of the esophagus consists of four layers, namely the mucosa, submucosa, muscularis externa, and adventitia. Its lumen is lined by several layers of stratified squamous epithelial cells (ECs) that act as a barrier or protective layer against the mechanical stresses produced by food bolus when food is ingested. Therefore, surface epithelialization of cell-scaffold constructs is considered to be the most important way to provide tissue-engineered substitutes with the natural esophageal functions.[6] Moreover, the basement membrane, a layer of acellular material underlining the epithelium, plays an important role in regulating the physical and biological activities of ECs and serves as an interface to keep them attaching to the lamina propia. In our previous study, the topological structure and extracellular matrix (ECM) protein contents (collagen IV, laminin, entactin, and proteoglycans) of porcine esophageal BM were analyzed. BM is a rugged and uneven strip with a thickness of 86 ± 15 nm. Its topology consists of interwoven fibers with mean diameter of 66 ± 24 nm (range 28−165 nm) and with abundant pores of unequal size.[7]

Recently, materials such as poly(lactide-co-glycolide) (PLGA), poly(L-lactic acid) (PLLA), polycaprolactone (PCL), and poly(L-lactide-co-caprolactone) (PLLC) have been used to fabricate scaffolds with the aim of promoting esophageal tissue regeneration by supporting the growth of esophageal smooth muscle cells (SMCs), fibroblasts and epithelial cells (ECs).[8−12] On the other hand, using poly(ester urethane) (PU) as the matrix, tubular scaffold with microchannels of 100 μm width and discontinuous channel wall with gaps of 30 μm (Prototype 1) in the lumen and microchannels of 200 μm width and continuous channel walls (Prototype 2) on the exterior was fabricated, resulting in regenerating muscle tissue with endocircular and exolongitudinal esophageal muscle architecture.[13]

Silk fibroin (SF), a fibrous protein in the core region of silk, has been investigated in a variety of biomedical applications such as tissue scaffold and tissue regeneration due to its

Received: December 27, 2013
Accepted: March 18, 2014
Published: March 28, 2014

   dx.doi.org/10.1021/am4059809 | ACS Appl. Mater. Interfaces 2014, 6, 4954−4964

favorable mechanical properties and biocompatibility. It has been verified that SF played an important role in enhancing cell adhesion, migration, proliferation and differentiation in cell culturing when it was included in scaffolds.[14,15] In this work, we focus on replicating an artificial epithelium with nanofibrous scaffold prepared from polycaprolactone (PCL) and silk fibroin (SF) using electrospinning technology, separately and combined. To enhance the biological activities of the cultured ECs, we extracted major BM proteins including collagen IV, laminin, entactin, and proteoglycans from porcine mucosal tissue and coated onto the surface of PCL/SF scaffolds. EC behaviors were evaluated by in vitro culturing of primary esophageal ECs on scaffolds. The biocompatibility and epithelium regeneration capability of the scaffolds were investigated through subcutaneous embedding as well as in situ implantation in the esophagus using rabbits as the experimental animal. Results demonstrated that both PCL/SF and BM protein-coated scaffolds provided favorable environment for EC's in vitro growth and differentiation, as well as in vivo wound recovery and epithelium regeneration. Therefore, porous and fibrous scaffolds prepared under the protocol presented in this work can be considered as suitable artificial BM substitutes for promoting epithelium regeneration.

2. MATERIALS AND METHODS

2.1. Materials. Polycaprolactone (PCL, M_n 80 000) was purchased from Sigma-Aldrich Co., USA. Poly (ester urethane) (PU, 58213 NAT 022) was purchased from Estane Co., China. 1,1,1,3,3,3-hexafluoro-2-propanol (HFIP) and trifluoroethanol (TFE) were purchased from Shanghai Darui Fine-chemical Co., China. Formic acid (FA) was purchased from Sinopharm Chemical Reagent Co., China. Dulbecco's modified Eagle's medium (DMEM), fetal bovine serum (FBS) and antibiotic antimycotic solution (AAS, 100 IU mL^{-1} penicillin, 100 μg mL^{-1} streptomycin and 0.25 μg mL^{-1} amphotericin B) were purchased from Gibco (Invitrogen Co., USA). Antihuman CK14 was purchased from Santa Cruz Biotechnology In., Europe. FITC- or Rhodamine-conjugated goat antimouse IgG (H+L) antibodies were purchased from Beijing Biosynthesis Biotechnology Co., China. All chemical reagents used for western-blotting were purchased from Beyotime Institute of Biotechnology, China. Other chemical reagents were from Sinopharm Chemical Reagent. Water used in the experiment was deionized water provided from MilliPore Pure Water Machine (7146, Thermo Scientific Co., USA). Phosphate buffer saline (PBS) used in cell culture was sterilized.

2.2. Extraction of Silk Fibroin (SF). Silk fibroin was extracted from the natural silkworm cocoons (Zhejiang Province, China) using a previously characterized method.[16] The cocoons were boiled for 1 h in an aqueous Na_2CO_3 solution (0.5 wt %) and rinsed with water to remove the sericin. The extracted fibers were then dissolved in calcium nitrate tetrahydrate ($Ca(NO_3)_2{\cdot}4H_2O$) at 80 °C to yield a homogeneous solution (5 wt %) and subsequently dialyzed against water for 3 d at room temperature (RT) using cellulose tubular membrane (MW cutoff, 12 000−14 000, Sigma-Aldrich Co., USA). Water was changed every 4 h to completely remove residual salts. The resulting solution was freeze-dried to obtain silk fibroin sponge.

2.3. Extraction of BM Proteins and Coating on Scaffold. BM protein extracts were prepared using the method described previously.[7] In brief, the mucosa and submucosa layers of fresh porcine esophagus were minced, homogenized in high-speed Dispensator (XHF-D, Ningbo Scientz Biotechnology Co., China) and extracted sequentially in the following solutions: (1) 3.4 M NaCl, 0.05 M Tris−HCl, protease inhibitor (2 mM phenylmethylsulfonyl fluoride, 1 mM N-methylmaleimide); (2) 0.5 M NaCl, 0.05 M Tris−HCl, protease inhibitor. The obtained mixture was centrifuged (8,000 g, 20 min) at 4 °C. The supernatant was then collected and its protein concentration was determined before being stored at −20 °C for the following application.

Electrospun PCL/SF scaffolds were immersed in the BM protein extracts for 24 h at RT. The scaffold was then rinsed with PBS for three times to remove unbound proteins and dried in vacuum oven overnight. PCL/SF soaked in PBS only was used as reference.

2.4. Scaffold Preparation. PCL and SF were dissolved in TFE and FA, respectively. PCL/SF (4:1, w:w) were dissolved in 1,1,1,3,3,3-hexafluoro-2-propanol (HFIP) at the concentration of between 0.10 and 0.25 g/mL. Scaffolds were fabricated using the electrospinning system setup by our laboratory (China patent ZL 2008 1 0062323.8). Prepared polymer solutions were loaded into a 20-mL plastic syringe controlled by a syringe pump and fixed onto an insulated movable stage. Electrospinning was performed with the applied voltage of 15−30 kV using a high-voltage power supply (Hangzhou Qiaofeng Electrostatic Equipments Factory, China). A grounded planar stainless steel collector was located at a distance of 7−11 cm from the needle tip. The diameter of needle tip was 0.7 mm. Polymer solution was fed into the needle tip at the rate of 0.2−1.5 mL/h. A positively charged polymer jet formed from the Taylor cone at the nozzle of the needle and discharged onto the grounded collector under the combined force of gravity and electrostatic charge. Electrospun fibers were collected and observed by microscopy to determine electrospinning parameters. Two types of collector substrates were used; tinfoil was used for morphological characterization while circular glass slides (diameter 14 mm) were used for in vitro cell culture. The process parameters were listed in Table 1.

Table 1. List of Electrospinning Parameters for Scaffold Preparation

sample	solvent	concentration (g/mL)	voltage (kV)	distance (cm)
PCL	TFE	0.13	25	10
PCL/SF	HFIP	0.12 (4/1)[a]	20	8.5
SF	FA	0.15	15	9.0

[a]The ratio of PCL to SF, w/w.

Scaffolds used for cell culture experiments were sterilized by immersion in 75% alcohol for 4 h and rinsed in sterile PBS to remove residual alcohol. The sterilized scaffolds were then immersed in DMEM for 30 min and placed in 24-well tissue culture polystyrene plates (TCPS, Corning Incorporated, USA).

2.5. Scaffold Characterization. *2.5.1. Scanning Electron Microscopy (SEM).* To determine the morphology of the electrospun fibers, we gold-coated the samples using an auto fine coater (Hitachi, E-1010, Japan) and examined them under a scanning electron microscope (SEM, Hitachi, S-3400N, Japan) at an acceleration voltage of 10 kV. Image J 1.41o software (Wayne Rasband, National Institutes of Health, USA) was used to measure the diameters of the electrospun fibers. The average diameter was determined by randomly measuring at least 30 fibers from each SEM image and is expressed as mean ± standard deviation (SD). Three random SEM images were used for each sample.

2.5.2. Mechanical Property Test. Mechanical testing was performed with a linear tensile tester (Instron 3366, USA). The scaffold samples were cut into dumbbell shape of 20 mm gauge length with cross-section dimensions of 0.1 mm ×0.3 mm ×10 mm. The samples were linearly deformed at the rate of 1.0 mm/min. The mechanical properties of PCL, SF, and PCL/SF (4:1, w:w) scaffolds were separately tested. Three samples were tested for each scaffold type. The scaffolds were sterilized in 75% alcohol for 2 h, rinsed in PBS to remove residual alcohol and kept in PBS solution prior to the evaluation of their mechanical properties.

2.5.3. Degradation Test. The scaffolds were sterilized in 75% alcohol for 2 h, and rinsed in water to remove the residual alcohol. After drying in vacuum oven, samples were incubated in PBS (pH 7.4) supplemented with 100 U/mL Penicillin-streptomycin at 37 °C. Prior to weight measurement on an electronic analytical balance (Sartorius BS 224s, Germany), samples were rinsed in water and dried in vacuum oven. The percentage of weight loss after different time periods (1, 3, 7, 15, 30, and 60 days) was calculated using the following formula

$$\text{weight loss}\ (\%) = \frac{W_0 - W_1}{W_0} \times 100\%$$

W_0 represents the initial weight of the sample (mg); W_1 represents the measured weight (mg) of the same sample after different degradation time. The degradation tests were conducted in triplicates for each time point.

2.5.4. Immunohistochemical Staining. The BM protein coated PCL/SF (coated-PCL/SF) fibers was immunohistochemistry analyzed with uncoated PCL/SF as the negative control. The samples were fixed in 4% formaldehyde/PBS for 24 h at 4 °C, followed by dehydration through a graded series of alcohol, transparency with dimethylbenzene, wax-dipping and embedding in paraffin, section at 4 μm in microtome (Rotary Microtome HM 325, Thermo Scientific). Subsequently, they were dewaxed, hydrated, rinsed by PBS, and blocked in 4% normal goat serum for 2 h at room temperature. They were incubated in primary antibody of rabbit antilaminin (1:100) overnight at 4 °C. Sections were subsequently incubated in peroxidase-conjugated goat antirabbit IgG (1:1000) for 30 min followed by 3,3′-diaminobenzidine (DAB) incubation for 5 min at room temperature. Samples were observed in an optical microscopy.

2.6. Cell Culture. Primary epithelial cells (ECs) were isolated from fresh porcine esophagus tissue obtained from the local abattoir. Mucosal-submucosal layer of porcine esophagus was separated from the underlying connective tissue and rinsed in PBS supplemented with antibiotic antimycotic solution (AAS, 100 U/mL penicillin, 100 μg/mL streptomycin, and 100 U/mL Amphotericin B). The separated mucosal-submucosal layer was first sterilized in 1% H_2O_2 and then in 5% povidone iodine solution. It was subsequently incubated overnight in Dispase II/PBS solution (50 mg/mL) at 4 °C. The epithelium layer was minced after separation from the underlying lamina propia and further incubated in 0.5 wt % trypsin-EDTA (Genome, USA) at 37 °C for 20 min. The trypsin within the cell suspension was inactivated using an equal volume of DMEM containing 10% FBS. The minced epithelium was strained through a cell strainer and centrifuged at 1,500 rpm for 3 min at −4 °C (Eppendorf 5804R, Germany) to obtain a cell pellet. This cell pellet was resuspended in culture medium and cultured in a T-flask (Corning Incorporated, USA). High glucose DMEM supplemented with 10% FBS and AAS was used to culture the primary ECs. The culture medium was renewed every 2 days.

Cells from second to fourth passages were seeded on scaffolds at a density of 2.6×10^4 /cm^2 and were left undisturbed for 2 days to allow the cells to attach onto scaffolds. After culture for 14 days, cells were rinsed three times with PBS and fixed in 2.5 wt % glutaraldehyde solution for 30 min at RT followed by washing with distilled water. They were dehydrated sequentially by 30, 50, 70, 80, 90, 95, and 100% alcohol, with 10 min between each step. After gold coating, the cell morphology was observed under SEM at an accelerating voltage of 10 kV.

2.7. Mitochondrial Activity Assay. The mitochondrial activity of ECs on each scaffold was assessed using the MTT method. After the cultures were incubated in 3-(4,5-dimethylthiazol-2-yl)-2,5-Diphenyl-tetrazolium Bromide (MTT) solution (0.5 mg/mL) for 4 h at 37 °C in the dark, 400 μL of dimethylsulfoxide (DMSO) per culture well was used to dissolve the purple formazan crystal. Absorbance was measured at the wavelength of 490 nm by a photo spectrometer (MaxM5, Spectra). The absorbance of the DMSO without formazan crystal was also measured and used as blank reference. The absorbance values were compared among cells grown on PCL, PCL/SF, SF, coated-PCL/SF scaffolds, and TCPS well. Average absorbance was obtained by measuring each sample in triplicates.

2.8. Immunofluorescence Staining. The ECs cultured on scaffolds for 14 days were fixed in 4 wt % paraformaldehyde for 30 min at RT and rinsed trice with PBS for 10 min each time. The samples were first incubated in 0.1% Triton X-100 for 10 min, rinsed trice with PBS for 10 min each time, and subsequently blocked in blocking solution of 4% goat serum for 1h at RT to minimize nonspecific binding. The sample was drained off the blocking solution (without rinsing) and incubated overnight at 4 °C in anticytokeratin 14 (CK14) mouse monoclonal antibody (1:100 dilution in PBS). After rinsing with PBS, it was subsequently incubated in antimouse IgG (H+L) secondary antibody conjugated with FITC (1:100 dilution in PBS) for 1 h in dark. The sample was dipped in 4, 6-diamidino-2-phenylindole dihydrochloride (DAPI) solution (Sigma, 3 μg/mL in PBS) and rinsed with PBS to reveal the nuclei. In the stained image, EC's keratin displayed as green fluorescence and the nucleus displayed as blue.

2.9. Western-Blotting. ECs grown on scaffolds and TCPS (24-well plate) for 14 days were digested on ice for 30 min with 200 μL of Membrane and Cytosol Protein Extraction Kit (Beyotime Institute of Biotechnology, China) for each sample or well. The cell lysate was collected and centrifuged at 12 000 rpm for 5 min. The supernatant was transferred to a new microcentrifuge tube for further analysis. About 20 μL supernatant, with 5 μL of loading buffer (5×), was loaded onto a 12% sodium dodecyl sulfate (SDS) polyacrylamide gel. Electrophoresis was performed in running buffer at 100 V for 2 h. The separated proteins were then electrically transferred onto a polyvinylidene fluoride membrane (PVDF, Roche Diagnostics). After blocking with 1% bovine serum albumin (BSA) for 1 h at RT, we incubated the membrane with antihuman CK14 (1:200 dilution in blocking solution) for 1 h at RT. After three washes of 15 min each time, the membrane was incubated with horseradish peroxidase-labeled antimouse antibody (Santa Cruz, dilution 1:2000) for 1 h at RT followed by addition of enhanced chemiluminescence (ECL) Western blotting detection reagents. Membranes were then exposed to light-sensitive film (Kodak Co., USA). The developed film was scanned with ImageJ. The relative levels of detected proteins were assessed by measuring the integrated intensity of all pixels in each band and subtracting the local background intensity. The results presented were obtained from at least three separate experiments.

2.10. In Vivo Testing of Scaffold'S Biocompatibility and Epithelium Regeneration. For in vivo experiments, PCL/SF was electrospun directly on the microchanneled PU using the same electrospinning parameters as above. The scaffolds were coated with BM protein extracts. To improve the wettability and biocompatibility and alleviate the harm of PU substratum, we grafted the PU surface with silk fibroin beforehand.[13]

New Zealand adult rabbits (1 year old, 4−6 kg) were anesthetized with 3% pentobarbital sodium (intravenous injection, 12 mg/kg). Scaffolds of coated-PCL/SF on PU substratum were implanted subcutaneously as shown in Figure 9a1. The inserted image is the implanted sample with diameter of 14 mm. The rabbits were kept at Animal Test Center of Ningbo University. After some days, the rabbits were anesthetized and the samples were harvested along with a small amount of surrounding tissue. The samples were fixed in 4% paraformaldehyde for 24 h at 4 °C and subsequently frozen at −80 °C. The frozen samples were sectioned at a slice with thickness of 5 μm using a freezing microtome machine (Hubei Bernard Medical Technology Co., BL-800A). These sections were processed with hematoxylin and eosin (H&E) staining and immunofluorescence staining.

All animals used in this study were handled in accordance with the requirements of the Ethics Committee of Ningbo University and National Institute of Health's Principles of Laboratory Animal Care.

2.11. Statistical Analyses. Data are expressed as mean ± standard deviation (SD). Statistical comparisons were made by analysis of variance (ANOVA). *t* test was used for evaluations of differences between groups. *P*-values less than 0.05 were considered to be significant.

3. RESULTS AND DISCUSSION

3.1. Properties of Electrospun Scaffolds. Electrospinning is an inexpensive method for producing nano/micro fibers by electrostatically drawing polymer solutions or polymer melts with the aim of fabricating scaffolds for tissue engineering research. As we aim to produce nanofibrous scaffolds to mimic the architecture of esophageal basement membrane, we selected polymer solution electrospinning. In this type of electrospinning, variables affecting fiber characteristics include

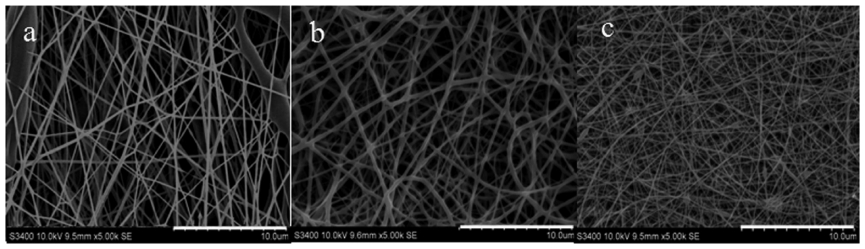

Figure 1. Fiber morphology of electrospun scaffolds observed under SEM, (a) PCL; (b) PCL/SF; (c) SF. Scale bar 10 μm.

concentration of polymer solution, solvent properties, applied voltage, distance between nozzle and collector, flow rate of solution, and the ambient conditions.[17−20] Herein, materials including PCL, PCL/SF, and SF were electrospun using the system parameters (Table 1), based on our previous work.[8,21,22] The morphologies of the electrospun fibers were observed under SEM (Figure 1). All electrospun fibers were found to be smooth with no observable coagulation. Although the pore and fiber sizes were different between different scaffold types, the pores on all scaffolds seemed to interconnect well. The fiber diameters of the PCL, PCL/SF, and SF scaffold were analyzed to be 140.2 ± 65.6 nm, 146.8 ± 60.6 nm, and 92.3 ± 28.7 nm, respectively, using ImageJ 1.41o software (Table 2, Figure 1).

Table 2. Quantitative Results of Scaffold Topologic Characters and Mechanical Properties

scaffold	diameter (nm)	σ (MPa)	ε (%)	E (MPa)
PCL	140.2 ± 65.6	1.6 ± 0.5	18.6 ± 0.8	13.5 ± 0.7
PCL/SF	146.8 ± 60.6	1.9 ± 0.3	26.2 ± 1.6	11.6 ± 1.0
SF	92.3 ± 28.7	2.9 ± 0.9	18.5 ± 1.3	37.2 ± 0.8

According to our prior experience, nanofibrous mesh scaffolds with topologies found in these three scaffolds are suitable to support the growth and proliferation of primary ECs.[8]

PCL, biodegradable aliphatic polyester, has been investigated for wide applications including drug delivery systems and tissue engineering scaffolds for skin, bone, esophagus, osteochondral, blood vessel, etc.[23−26] However, it is less favorable for EC growth as PCL is hydrophobic and does not have physiologically active site on its molecular chain. To ameliorate these disadvantages, PCL is often used in combination with natural biomaterials such as silk fibroin (SF), elastin, collagen, fibronectin, alginate, agarose, hyaluronic acid, chitosan, etc.[27−30] Previously, our group has included amounts of gelatin into PCL solution to modify its chemistry and improve its biocompatibility.[22] In this work, SF was electrospun individually and in combination with PCL.

As scaffolds must provide and retain sufficient mechanical strength during cell proliferation and tissue regeneration, these scaffolds were hence evaluated for their mechanical properties. Figure 2 shows the stress−strain characteristics of the electrospun PCL, PCL/SF and SF nanofibrous scaffolds. The ultimate stress (σ), maximum strain (ε), and Young's modulus (E) of the scaffolds are summarized in Table 2. SF scaffold exhibited the highest ultimate strength (also Young's modulus), whereas PCL scaffold is the lowest; PCL/SF scaffold was in between. However, PCL/SF displayed the highest maximum strain (Table 2). These findings are expected as SF has good mechanical strength while PCL has poor strength but good elasticity. When SF and PCL were mixed and electrospun together, the composite fibrous scaffold (PCL/SF) displayed

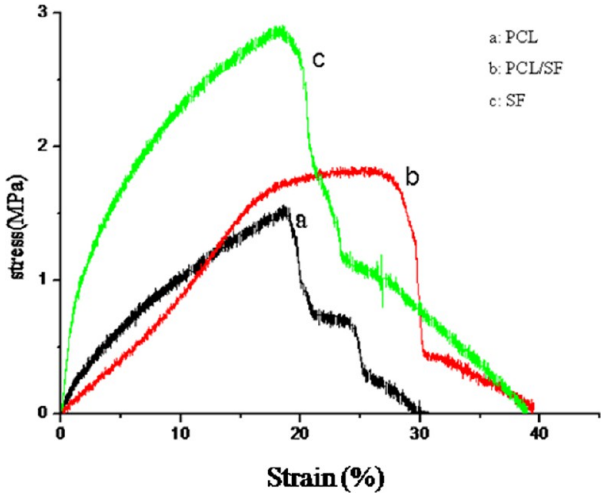

Figure 2. Tensile stress−strain curve of electrospun scaffolds. (a) PCL; (b) PCL/SF; (c) SF. Scaffolds were sterilized in 75% alcohol for 1 h and rinsed in PBS to remove alcohol before measurements.

both favorable strength and strain properties. Its ultimate tensile stress (1.9 ± 0.3 MPa) was similar to that of the acellular esophageal mucosa-submucosa matrix which was decellularized by surfactant combining with DNAase, i.e., (2.0 ± 0.84 MPa).[31] The use of SF, either individually or in combination with other polymers, can enhance the mechanical strength of nanofibrous scaffolds, whereas hybridization of SF and PCL can improve the strain characteristics of the prepared scaffold (PCL/SF).

An important consideration when designing scaffolds for tissue engineering applications is the degrading characteristics of a material, because the degradation rate of scaffolds should ideally match the growth rate of cell and tissue. For biodegradable polymers, the degradation usually occur in 4 steps; water sorption, reduction of mechanical properties (modulus and strength), reduction of molar mass and weight loss due to diffusing away the soluble oligomeric components.[32,33] Therefore, we tested the scaffold's degradation via weight loss measurements. The study of in vitro degradation may potentially help us to understand and predict the in vivo degradation behavior of these scaffolds. The in vitro degradation test was performed over a span of two months (Figure 3). For the initial 7 days of immersion in PBS at 37 °C, the weight loss of all scaffolds was negligible. Between 7 and 15 days, the PCL scaffold experienced a great weight loss of 18.6%; after then, little weight loss occurred until day 60. PCL is usually a slow degradation material and not good at fiber-forming itself.[21,22] PCL fibers are not as uniform in diameter as PCL/SF or SF fibers (the biggest standard error in Table 2). Some broken ends existed at some locations (data not shown). Literature[34] reported that the degradation pathway of PCL sheet is through surface degradation, resulting in an erosion of

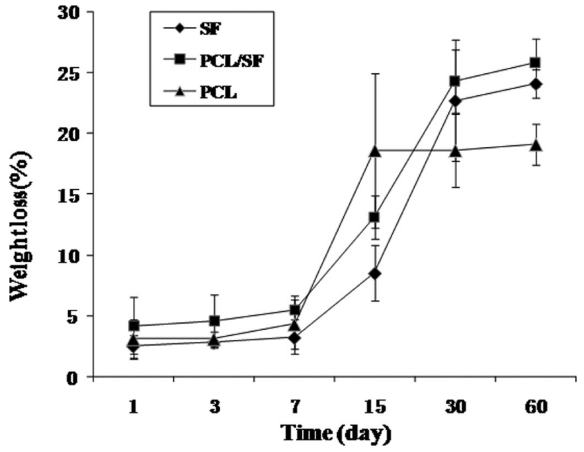

Figure 3. Scaffold's weight loss (%) as a function of time (day). Scaffolds were dipped for sometime at 37 °C in PBS (pH 7.4) supplemented with 100 U/mL penicillin-streptomycin. Samples were rinsed in water and dried in a vacuum oven at RT before weight measurements.

the scaffold bulk. In our case, the high weight loss of PCL sheet with high surface area (exhibited in SEM picture, Figure 1a) at the first stage might occur because of the diffusion of those super fine and broken ended fibers from the scaffold. After this kind of diffusion, PCL returned to be a slowly degradable material till the end of testing time. In contrast, the degradation of SF-containing scaffolds showed the different tendency. The sharp increase of weight loss occurred between 15 and 30 days, with the maximum loss of 24.1% for SF and 25.8% for PCL/SF over a 60 day span. From previous reports, the degradation behavior of silk fibroin was not only related to its crystallinity, but also to its hydrophilic interaction and crystalline-non-crystalline alternating nanostructures. The hydrophilic blocks of SF are degraded prior to the hydrophobic crystalline blocks.[35] It was expected that aqueous medium promoted hydrophilic degradation of SF. PCL/SF scaffold displayed similar degradation trend to SF. The degradation of PCL/SF scaffold was slightly faster than that of SF scaffold and a little faster than that of pure PCL scaffold after 30d. Basic salt residues, Na_2CO_3 or/and $Ca(NO_3)_2{\cdot}4H_2O$, left over the SF extraction process may potentially accelerate polyester (PCL) hydrolysis in aqueous medium to release its acidic element, which in turn further facilitates the SF degradation and thus resulted in the slightly highest degradation rate of PCL/SF during the whole tested span. Considering the mechanical properties (better flexibility) and degradation behaviors (blunt degradation at first 30 days), PCL/SF was selected to be the matrix for BM protein coating and in vivo tests.

3.2. BM Protein Coating on PCL/SF Nanofibrous Scaffold. Surface modification of nanofibers can improve the biocompatibility of artificial material/scaffold. Many biocompatibility studies focus on collagen coating on PCL nanofibers.[36−38] Collagen type IV is an essential component contributing to cell migration via providing epithelial cells with anchorage (primordial contacts), which was required for re-epithelialization of the denuded mucosa. Laminin is an important and biologically active part of the basal lamina, influencing cell adhesion, migration, and differentiation, as well as cell's phenotype and survival.[39] It forms an independent network and cross-links with the type IV collagen network via entactin, fibronectin, and perlecan.[7] Hence, to achieve a scaffold with favorable biocompatibility, PCL/SF nanofibrous scaffold was coated with BM protein extracts containing collagen IV, laminin, entactin, and proteoglycans. Figure 4 shows the surface

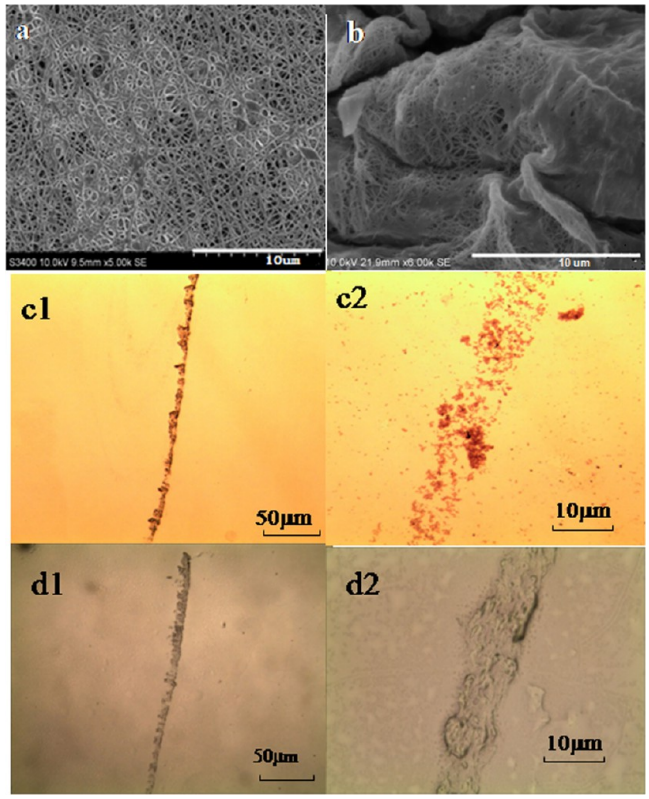

Figure 4. (a) SEM image after PCL/SF scaffold was coated by BM proteins that were extracted from porcine esophagus (coated-PCL/SF). Scale bar 10 μm. (b) Display of the BM topology. Reprinted with permission from ref 7. Copyright 2012 Wiley. (c, d) Immunohistochemical staining of cross-sections of coated-PCL/SF and PCL/SF sheet, using antilaminin as the primary antibody. (2) is the magnification of (1).

morphology of PCL/SF scaffold coated with BM proteins (coated-PCL/SF). The pores of coated-PCL/SF became merged due to protein coating (Figure 4a), which resembles the natural BM topology (Figure 4b[7]). Immunochemical staining of the coated-PCL/SF displayed a brown cross-section that was labeled with peroxidase using antilaminin as the primary antibody (Figure 4c). This result verified the presence of BM protein in coated-PCL/SF scaffold. Conversely, the uncoated PCL/SF scaffold did not show brown color as coated-PCL/SF did. ECs would be cultured on the SF, PCL/SF and coated-PCL/SF scaffolds to evaluate their suitabilities as substrates for re-epithelialization; PCL scaffold would be used as a negative control.

3.3. Growth and Differentiation of Epithelial Cells on Nanofibrous Scaffolds. Esophageal epithelium contains several layers of nonkeratinized stratified squamous epithelial cells and acts as a protective barrier against food, saliva and mucus transiting through it. From the basal layer (the bottom edge of nonkeratinized stratified squamous ECs abutting the basement membrane) to the lumen, epithelial cells can be divided into several layers like the basal, the spinous, and the superficial with different morphology and cytokeratin expression. As ECs migrate toward the lumen, they progressively become terminally differentiated and lose their proliferative

potential. Also, their morphology becomes flatter and larger.[40] To construct an artificial epithelium and promote EC differentiation, PCL and SF were electrospun in combination to fabricate nanofibrous scaffold. BM protein extracts were coated onto it for surface modification. Primary esophageal epithelial cells were cultured to evaluate the morphology, mitochondrial function and immunohistochemistry. After 14 days' culture, ECs attached onto the substrate fibers of PCL scaffold and were found to be growing in clusters (Figure 5a,

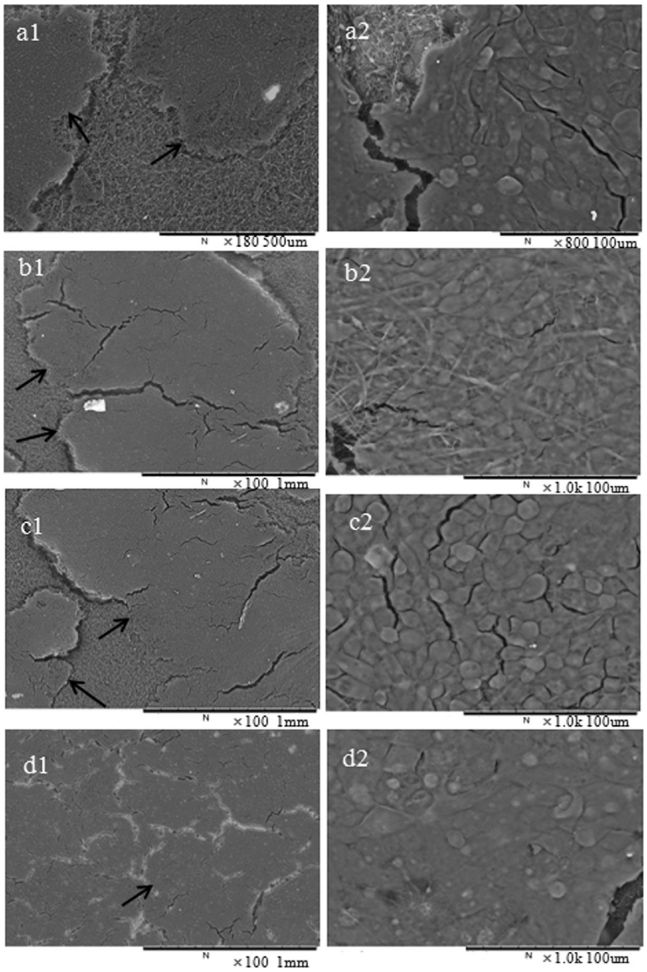

Figure 5. Cell morphology observed under SEM. ECs were seeded on the scaffolds of (a) PCL, (b) PCL/SF, (c) SF, and (d) coated-PCL/SF. Panels labeled 1 and 2 show different magnifications. Arrows indicated cell clusters in a, b, and c, and cell sheet in d. Cells were seeded at the density of 2.6×10^4 /cm^2 and cultured for 14 days at 37 °C in humidified air with 5% CO_2 (The same conditions were followed for all cell culture).

arrow) at low cell density relative to the entire seeding surface. But ECs were found to grow at higher total densities on both SF and PCL/SF scaffolds than that on PCL scaffold; ECs also exhibited the squamous epithelial phenotype (Figure 5b, c). On the coated-PCL/SF scaffold, ECs have achieved complete confluence and covered almost the entire scaffold surface (Figure 5 d1, arrow, and d2); the total EC number might be the highest among the all investigated scaffolds.

Quantitative analysis of the mitochondrial activity of ECs seeded on the test scaffolds demonstrated the similar tendency. Figure 6 shows that the relative mitochondrial activity (absorbance at 490 nm) increases for ECs cultured on all

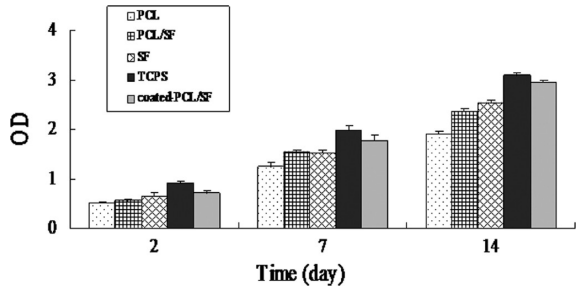

Figure 6. Mitochondrial activity assay. Cells were seeded at a density of 2.6×10^4 /cm^2 and cultured for 14 days.

scaffolds over 14d culture. The activity measured at day 2 reflects the ECs' ability to attach on different scaffolds. The attachment capabilities on the investigated substrates are as follows; PCL < PCL/SF < SF < coated-PCL/SF, with TCPS the highest. Protein components like SF or BM extracts on those scaffolds promoted the ECs' attachment capability. After culture for 7 and 14 days, ECs displayed similar viability trends on all scaffolds as those at day 2. Notably, the coated-PCL/SF scaffold greatly enhanced ECs' capabilities of attachment and proliferation (the highest absorbance at day 2 and day 14 except for TCPS). These results were completely consistent with the results observed under SEM.

Cytokeratins are proteins of keratin-containing intermediate filaments found in the intracytoplasmic cytoskeleton of epithelial tissue. There are acidic type I and basic or neutral type II cytokeratins. Ck14 is a member of the type I keratin family of intermediate filament proteins. It is usually found as a heterodimer with type II keratin 5 and forms the cytoskeleton of epithelial cells.[41,42] Although it displays cell morphology via immune-fluorescence, the expression of CK14 can also be used as an index to epithelial cells' differentiation. After being cultured for 14 days, ECs on scaffolds were immunofluorescence stained with anti-CK 14 to reveal the cell phenotype and differentiation, and to confirm the epithelial origin. Figure 7 shows the fluorescence images of nuclei (1, blue), cytokeratin (2, green), and their composite (3). The cells on all scaffolds were verified to be squamous EC from the green florescence shown in Figure 7a2, b2, c2, and d2. The general cell densities on PCL/SF and SF scaffolds were comparatively higher (Figure 7 b, c) than that on pure PCL scaffold (Figure 7a). ECs cultured on the coated-PCL/SF scaffold not only displayed epithelial phenotype (Figure 7d). It also has reached confluence to cover the whole scaffold surface, which was in agreement with the appearance of SEM observation (Figure 5d, arrow).

The western-blotting results were exhibited in Figure 8. Bands from left to right represent the CK14 expression of EC on PCL, PCL/SF, SF, coated-PCL/SF, and TCPS, respectively, with its optical intensity gradually increasing in this order (Figure 8a). Figure 8b shows the optical density (normalized to TCPS) and indicates that ECs cultured on coated-PCL/SF had significantly higher levels of CK14 expression than that of ECs cultured on PCL scaffold, but was slightly less than that of ECs on TCPS. The optical intensities on PCL/SF and SF were in between. This result was in accordance with the visual survey of SEM observation and immunofluorescence staining. In a word, coated-PCL/SF possessed the best cytocompatibility to primary epithelial cells among all tested scaffolds, i.e., PCL, PCL/SF, SF, and coated-PCL/SF. BM protein coating greatly promotes the interaction between ECs and scaffolds. Thus, we

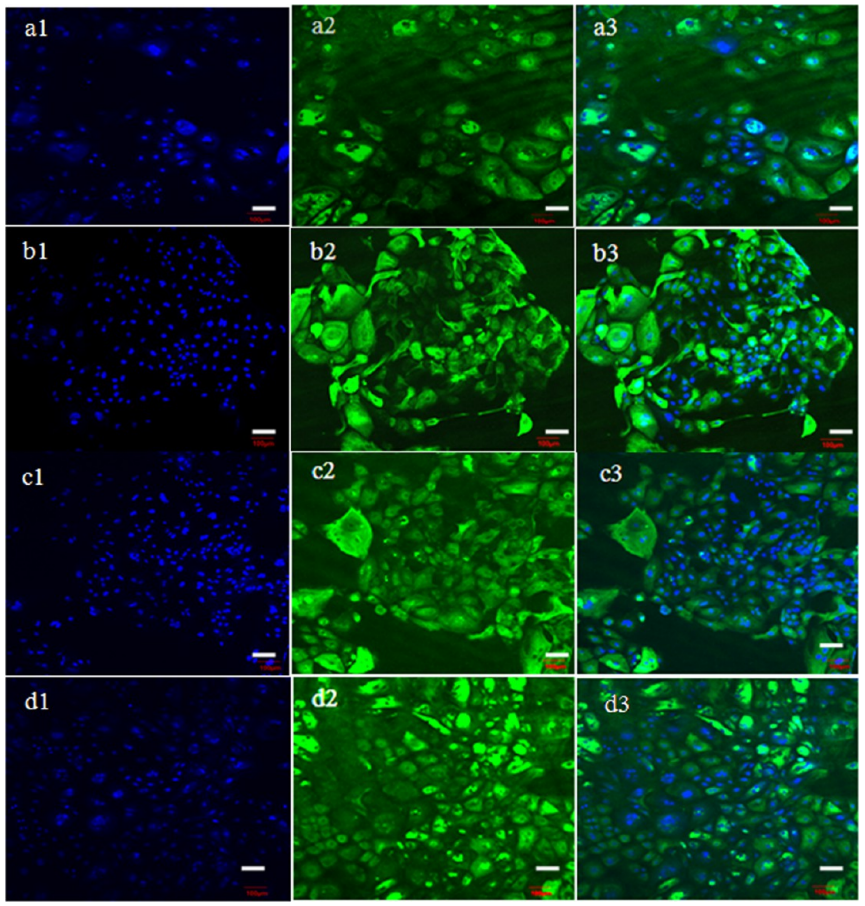

Figure 7. Cell phenotype. Cells on scaffolds were immunohistochemically stained with CK14 antibody. The nuclei were stained with DAPI to display blue (1) and the keratin was stained with anti-CK14 to display green (2); (3) is the composite of (1) and (2). (a) PCL, (b) PCL/SF, (c) SF, and (d) coated-PCL/SF. Cells were seeded at a density of 2.6×10^4 /cm^2 and cultured for 14 days. Scale bar 100 μm.

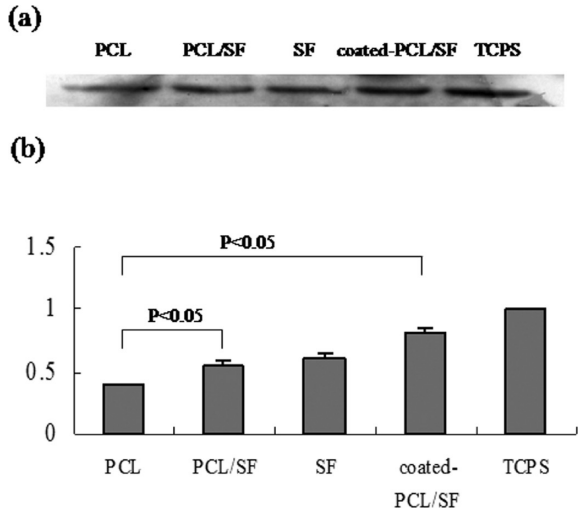

Figure 8. Expression of CK14 keratin on scaffolds measured by western-blotting method. (a) Stripes from left to right represent the CK14 expression on PCL, PCL/SF, SF, coated-PCL/SF, and TCPS, respectively, after they were cultured in vitro for 14 days. (b) Quantitative analysis of CK14 expression (results were normalized by TCPS). *P*-value is <0.05.

would investigate the in vivo behaviors of the coated-PCL/SF scaffold via subcutaneous implantation and in situ esophagus substitution.

3.4. In Vivo Tests of Scaffold Biocompatibility and Epithelium Regeneration. In our previous work, a PU scaffold with microchannel patterns was verified to promote esophageal smooth muscle cell (SMC) growth and differentiation after it was grafted with silk fibroin.[13] In this work, this PU scaffold was used as a physical support, on which PCL/SF (4:1, w:w) fibers were electrospun and BM proteins were coated, aiming at achieving a good scaffold for epithelium regeneration. First, coated-PCL/SF on PU membrane was implanted into rabbit's hypodermis to evaluate the scaffold's in vivo biocompatibility. Postoperatively, inflammation occurred during the first 3 days, but was markedly reduced at day 7. The wound had completely recovered by day 30 while hair regenerated normally by day 45 (Figure 9a2, a3). Then we cut open the skin and exposed the sample location. At day 30 after the implantation operation, the subcutaneous scaffolds were already enclosed in the skin hypodermis, but displayed a little inflammation and blood swelling at the scaffold's circumference (Figure 9b1). At day 45, inflammation at the implantation site was significantly reduced (Figure 9b2) and completely resolved at day 80 (Figure 9b3). There was angiogenesis around the scaffold, which was supposed to promote the scaffolds' biocompatibility. H&E staining revealed that the electrospun sheet existed obviously above the PU support, on which new/regenerated tissue had grown at days 30 and 45 (Figure 9c1, c2, arrow). The electrospun sheet became thinner because of the degradation as more fresh tissue

dx.doi.org/10.1021/am4059809 | ACS Appl. Mater. Interfaces 2014, 6, 4954−4964

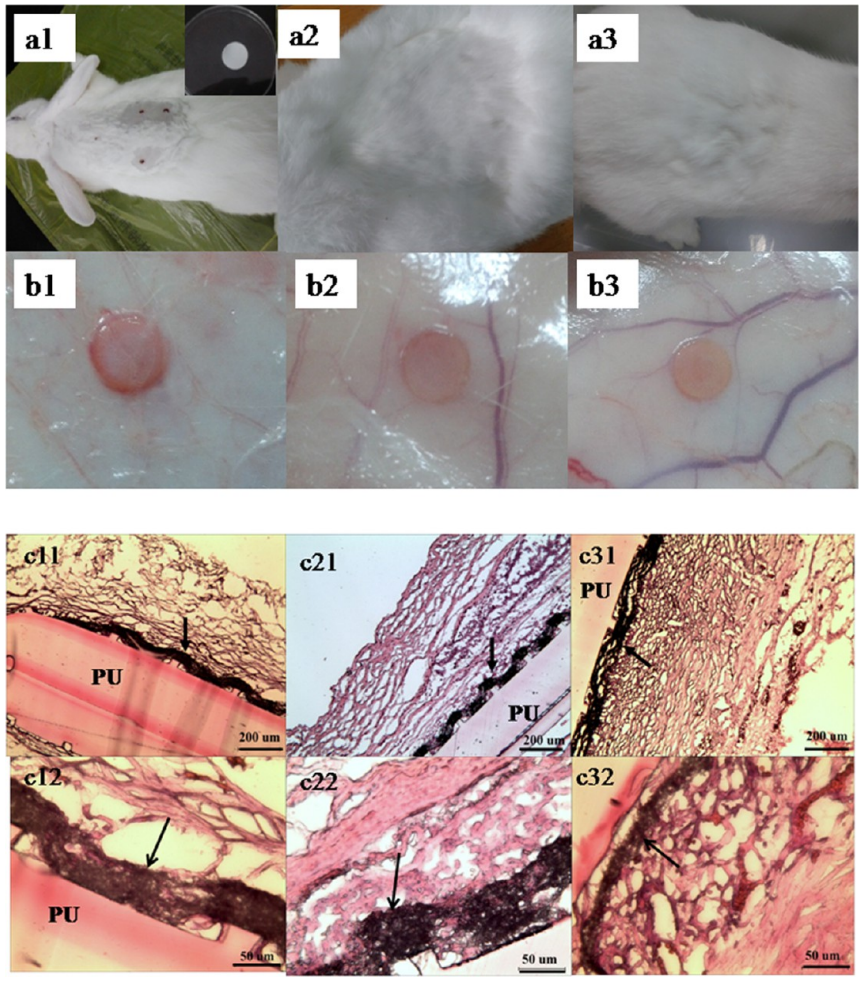

Figure 9. Top: (a1) Overview image of rabbits' back after scaffold sheet with diameter of 14 mm (the inserted) was implanted subcutaneously. (a2, a3) Overviews of wound recovery after 30 and 45 days of the operation, respectively. (b) Overviews of scaffolds encapsulated in tissue after they were implanted for (1) 30, (2) 45, and (3) 80 days, respectively. Bottom: H & E staining of the subcutaneous scaffolds after they were implanted for (c1) 30, (c2) 45, and (c3) 80 days, respectively. (2) is the magnification of (1). Arrow indicated the electrospun strip. The electrospinning was performed on PU substratum.

grew over the scaffold at day 80 than those at day 30 and 45 (Figure 9c3, arrow).

After verifying the biocompatibility, scaffold's mucosal regeneration capability was evaluated via in situ defect repairing experiment. A defect of approximately 5 × 5 mm was created at the middle of rabbit's esophagus and a coated-PCL/SF scaffold (together with PU substrate) of similar size was implanted at the defected site (Figure 10a, inserted). After 45 days, the rabbits were sacrificed and the esophagus lumen was exposed to show the implant site (Figure 10b, black thread). A brief visual inspection revealed that the mucosa had completely regenerated over the scaffold at the lumen defect. H&E staining for the implanted electrospun scaffold revealed that the entire wound were covered by newly regenerated tissue (Figure 11 a1). Newly regenerated epithelium was found to have grown along the surface of the electrospun scaffold and was thicker at the proximal end while thinner at the middle (Figure 11a1, arrow). The electrospun scaffold was also observed to have degraded as it has become thinner than the original implanted scaffold (Figure 11a2), which was coincident to the results of the subcutaneous experiment (Figure 9). Simultaneously, the epithelium was regenerating along the esophagus lumen. The newly regenerated epithelium was thinner at the distal end (Figure 11 b1, arrow) and thicker at the proximal end (Figure 11b2) at day 80. However, both regenerated epitheliums were not the same thickness as the normal esophagus (Figure 11a0). Unexpectedly, the scaffold was found to have degraded into fragments (Figure 11 b2, triangle), which was not observed during in vivo subcutaneous testing at day 80. The accelerated degradation/fragmentation of the scaffold may have been due to the mechanical stress induced during food ingestion and digestive enzymes brought by food bolus from mouth cavity or the occasional backflow of gastric fluids from stomach or both

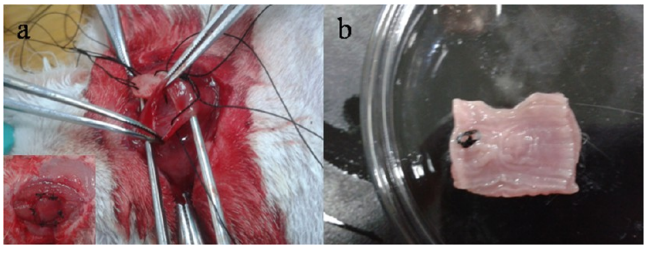

Figure 10. (a) Operation of scaffold in situ implantation and (b) the overview of the mucosa appearance after implantation for 80 days.

dx.doi.org/10.1021/am4059809 | ACS Appl. Mater. Interfaces 2014, 6, 4954−4964

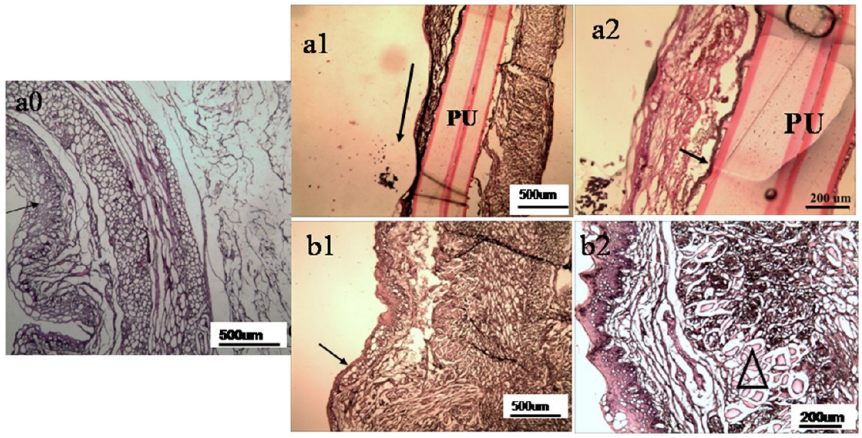

Figure 11. H&E staining of the in situ implanted scaffolds after 45 days (a1 and a2, arrow directed the epithelium regeneration in a1 and electrospun strip in a2) and 80 days (b1 and b2, arrow indicated the epithelium and triangle indicated the scaffold fragments). (a0) is the normal esophagus used as a reference (arrow means the esophagus lumen).

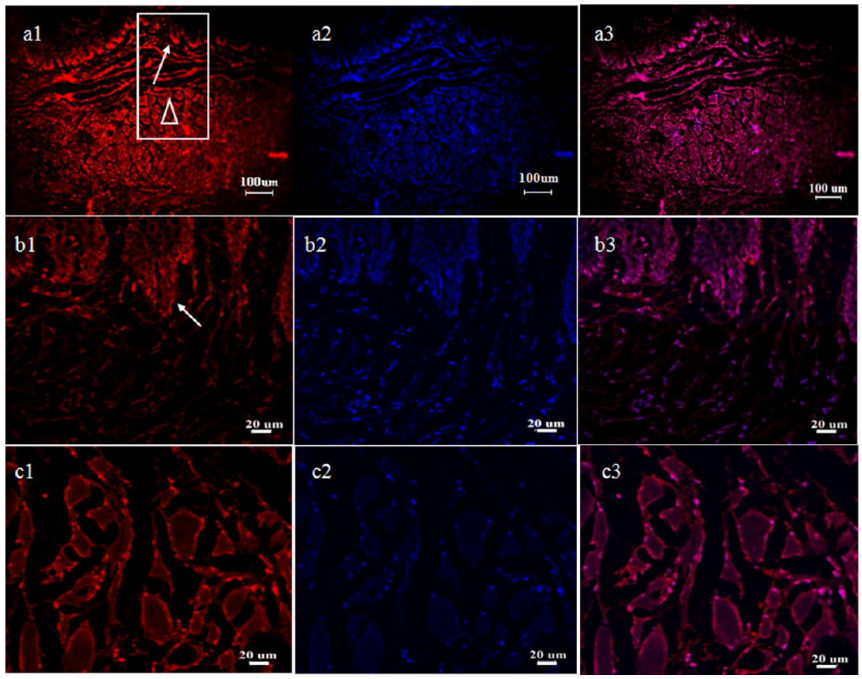

Figure 12. Immunofluorescence staining of the in situ implanted scaffolds after 80 days. Anti-CK14 was used as the primary antibody. (a) Regenerated mucosa with low magnification, arrow indicated the epithelium and triangle indicated the scaffold fragments; (b, c) magnified from square site of (a). The keratin was stained with anti-CK14 to display red (2) and nuclei were stained with DAPI to display blue (1), (3) is the composite of (1) and (2).

causes. Immunofluorescence staining using CK 14 as the primary antibody confirmed the cells as epithelial cells (Figure 12a, b, arrow). From the magnified image, scaffolds were found to have broken into fragments (Figure 12c1, magnified from triangle site of a1) and some cells infiltrated and encircled on the fragment's periphery (Figure 12c2, blue nuclei). The broken pieces also displayed red due to material's adsorption of red fluorescence. These founds were in accordance with those of H&E staining results (Figure 11). These all results convinced us that the coated-PCL/SF scaffold possessed favorable biocompatibility and might be used as a potential candidate for repair of epithelium defect. Further in vivo study is currently being performed in our group.

4. CONCLUSIONS

In this work, several types of nanofibrous scaffolds, PCL, PCL/SF, SF, and coated-PCL/SF, were prepared using electrospinning technology. The morphology, mechanical properties, and degradation behaviors of all scaffolds were tested and evaluated. The introduction of natural fibrous protein, SF, optimized the scaffolds' physical and chemical properties, but slightly accelerated the scaffolds' degradation. To construct an artificial BM capable of promoting epithelium regeneration, BM major proteins including collagen IV, laminin, entactin and proteoglycans were extracted from esophagus tissue and coated onto these nanofibrous scaffold. After evaluating the ECs' morphology, mitochondrial activity, immunohistochemistry, and Western blotting, the coated-PCL/SF scaffold was verified to have the best proliferation and differentiation to porcine

primary epithelial cells. Using PU scaffold as the physical support, the in situ implantation test revealed that the coated-PCL/SF possessed good biocompatibility and capability to promote regeneration of defected epithelium. These results provide evidence that ECM protein coating on electrospun PCL/SF would be a promising and practicable method to construct an artificial BM aiming at epithelium regeneration. Long-term in vivo study on epithelium defect repairing and further the whole esophagus restoring are currently being performed in our group.

AUTHOR INFORMATION

Corresponding Author

*E-mail: zhuyabin@nbu.edu.cn. Tel: +86-0574-87609592. Fax: +86-0574-87608638.

Notes

The authors declare no competing financial interest.

ACKNOWLEDGMENTS

The authors gratefully acknowledge the financial support from the National Science Foundation (81171476), Natural Science Funds for Distinguished Youth Team of Zhejiang Province (R2101166), and Scientific Innovation Team Project of Ningbo (2011B82014), China. This work was also sponsored by K. C. Wang Magna Fund of Ningbo University.

REFERENCES

(1) Pisani, P.; Parkin, D. M.; Bray, F.; Ferlay, J. Estimates of the Worldwide Mortality from 25 Cancers in 1990. *Int. J. Cancer* **1999**, *83*, 18−29.

(2) Parkin, D. M.; Bray, F.; Ferlay, J.; Pisani, P. Global Cancer Statistics, 2002. *CA Cancer J. Clin.* **2005**, *55*, 74−108.

(3) Ekman, S.; Dreilich, M.; Lennartsson, J.; Wallner, B.; Brattström, D.; Sundbom, M.; Bergqvist, M. Esophageal Cancer: Current and Emerging Therapy Modalities. *Expert Rev. Anticancer Ther.* **2008**, *8*, 1433−1448.

(4) Daly, J. M.; Fry, W. A.; Little, A. G.; Winchester, D. P.; McKee, R. F.; Stewart, A. K.; Fremgen, A. M. Esophageal Cancer: Results of an American College of Surgeons Patient Care Evaluation Study. *Am. Coll. Surg.* **2000**, *190*, 562−573.

(5) Enzinger, P. C.; Mayer, R. Esophageal Cancer. *N. Engl. J. Med.* **2003**, *349*, 2241−2252.

(6) Sato, M.; Ando, N.; Ozawa, S.; Miki, H.; Hayashi, K.; Kitajima, M. Artificial Esophagus. *Mater. Sci. Forum* **1997**, *250*, 105−114.

(7) Li, Y. Y.; Zhu, Y. B.; Yu, H. W.; Chen, L.; Liu, Y. X. Topographic Characterization and Protein Quantification of Esophageal Basement Membrane for Scaffold Design Reference in Tissue Engineering. *J. Biomed. Mater. Res. B: Appl. Biomater.* **2012**, *100*, 265−273.

(8) Zhu, Y. B.; Leong, M. F.; Ong, W. F.; Chan-Park, M. B.; Chian, K. S. Esophageal Epithelium Regeneration on Fibronectin Grafted Poly(L-lactide-co-caprolactone) (PLLC) Nanofiber Scaffold. *Biomaterials* **2007**, *28*, 861−868.

(9) Zhu, Y. B.; Chian, K. S.; Chan-Park, M. B.; Mhaisalkar, P. S.; Ratner, B. D. Protein Bonding on Biodegradable Poly(l-lactide-co-caprolactone) Membrane for Esophageal Tissue Engineering. *Biomaterials* **2006**, *27*, 68−78.

(10) Zhu, Y. B.; Chan-Park, M. B. Density Quantification of Collagen Grafted on Biodegradable Polyester: its Application to Esophageal Smooth Muscle Cell. *Anal. Biochem.* **2007**, *363*, 119−127.

(11) Zhu, Y. B.; Ong, W. F. Epithelium Regeneration on Collagen (IV) Grafted Polycaprolactone for Esophageal Tissue Engineering. *Mater. Sci. Eng., C* **2009**, *29*, 1046−1050.

(12) Zhu, Y. B.; Ong, W. F.; Chan, W. Y.; Li, Y. Y.; Liu, Y. X. Construct of Asymmetrical Scaffold and Primary Cells for Tissue Engineered Esophagus. *Mater. Sci. Eng., C* **2010**, *30*, 400−406.

(13) Gong, C. F.; Hou, L.; Zhu, Y. B.; Lv, J. J.; Liu, Y. X.; Luo, L. In vitro Constitution of Esophageal Muscle Tissue with Endocyclic and Exolongitudinal Patterns. *ACS Appl. Mater. Interfaces* **2013**, *5*, 6549−6555.

(14) Sofia, S.; McCarthy, M. B.; Gronowicz, G.; Kaplan, D. L. Functionalized Silk-based Biomaterials for Bone Formation. *J. Biomed. Mater. Res.* **2001**, *54*, 139−148.

(15) Kim, H. J.; Kim, U. J.; Kim, H. S.; Li, C.; Wada, M.; Leisk, G. G.; Kaplan, D. L. Bone Tissue Engineering with Premineralized Silk Scaffold. *Bone* **2008**, *42*, 1226−1234.

(16) Mathur, A. B.; Tonelli, A.; Rathke, T.; Hudson, S. The Dissolution and Characterization of Bombyx Mori Silk Fibroin in Calcium Nitrate-methanol Solution and the Regeneration of Films. *Biopolymers* **1997**, *42*, 61−74.

(17) Pham, Q. P.; Sharma, U.; Mikos, A. G. Electrospun Poly (ε-caprolactone) Microfiber and Multilayer Nanofiber/microfiber Scaffolds: Characterization of Scaffolds and Measurement of Cellular Infiltration. *Biomacromolecules* **2006**, *7*, 2796−2805.

(18) Haghi, A. K.; Akbari, M. Trends in Electrospinning of Natural Nanofibers. *Phys. Status Solidi A* **2007**, *204*, 1830−1834.

(19) Chong, E. J.; Phan, T. T.; Lim, I. J.; Zhang, Y. Z.; Bay, B. H.; Ramakrishna, S. Evaluation of Electrospun PCL/gelatin Nanofibrous Scaffold for Wound Healing and Layered Dermal Reconstitution. *Acta Mater.* **2007**, *3*, 321−330.

(20) Szentivanyi, A.; Chakradeo, T.; Zernetsch, H.; Glasmacher, B. Electrospun Cellular Microenvironments: Understanding Controlled Release and Scaffold Structure. *Adv. Drug Delivery Rev.* **2011**, *63*, 209−220.

(21) Zhu, Y. B.; Cao, Y.; Pan, J.; Liu, Y. X. Macro-alignment of Electrospun Fibers for Vascular Tissue Engineering. *J. Biomed. Mater. Res. B* **2010**, *92B*, 508−516.

(22) Zhu, Y. B.; Li, Y. Y.; Liu, Y. X. Fabrication of Gelatin and Polycaprolactone Composite Fibers using Electrospinning Technology. *Chin. J. Ningbo Univ. (NSEE)* **2009**, *22*, 408−413.

(23) Lee, J. S.; Go, D .H.; Bae, J. W.; Lee, S. J.; Park, K. D. Heparin Conjugated Polymeric Micelle for Long-term Delivery of Basic Fibroblast Growth Factor. *J. Controlled Release* **2007**, *117*, 204−209.

(24) Erisken, C.; Kalyon, D. M.; Wang, H. Functionally Graded Electrospun Polycaprolactone and β-tricalcium Phosphate Nanocomposites for Tissue Engineering Applications. *Biomaterials* **2008**, *29*, 4065−4073.

(25) Powell, H. M.; Boyce, S. T. Engineered Human Skin Fabricated using Electrospun Collagen−PCL Blends: Morphogenesis and Mechanical Properties. *Tissue Eng., Part A* **2009**, *15*, 2177−2187.

(26) Chen, H.; Huang, J.; Yu, J.; Liu, S.; Gu, P. Electrospun Chitosangraft-poly(ε-caprolactone)/poly (ε-caprolactone) Cationic Nanofibrous Mats as Potential Scaffolds for Skin Tissue Engineering. *Int. J. Biol. Macromol.* **2011**, *48*, 13−19.

(27) Um, I. C.; Fang, D.; Hsiao, B. S.; Okamoto, A.; Chu, B. Electrospinning and Electro-blowing of Hyaluronic Acid. *Biomacromolecules* **2004**, *5*, 1428−1436.

(28) Greiner, A.; Wendorff, J. H. Electrospinning: a Fascinating Method for the Preparation of Ultrathin Fibers. *Angew. Chem., Int. Ed.* **2007**, *46*, 5670−5703.

(29) Ekaputra, A. K.; Prestwich, G. D.; Cool, S. M.; Hutmacher, D. W. The Three-dimensional Vascularization of Growth Factor-releasing Hybrid Scaffold of Poly (ε-caprolactone)/collagen Fibers and Hyaluronic Acid Hydrogel. *Biomaterials* **2011**, *32*, 8108−8117.

(30) Annabi, N.; Fathi, A.; Mithieux, S. M.; Martens, P.; Weiss, A. S.; Dehghani, F. The Effect of Elastin on Chondrocyte Adhesion and Proliferation on Poly (ε-caprolactone)/elastin Composites. *Biomaterials* **2011**, *32*, 1517−1525.

(31) Yu, J. Y.; Zhu, Y. B.; Li, Y. Y.; Dong, W.; Xuan, F.; Mao, J. H.; Gong, C. F. Fabrication and Mechanical Properties of Decellularized Esophageal Submucosal Matrix. *Chin. J. Biomed. Eng.* **2010**, *30*, 312−315.

(32) Hakkarainen, M.; Albertsson, A. C.; Karlsson, S. Weight Losses and Molecular Weight Changes Correlated with the Evolution of

Hydroxyacids in Simulated *in vivo* Degradation of Homo- and Copolymers of PLA and PGA. *Polym. Degrad. Stab.* **1996**, *52*, 283−291.
(33) Göpferich, A. Mechanisms of Polymer Degradation and Erosion. *Biomaterials* **1996**, *17*, 103−114.
(34) Lam, C. X.; Hutmacher, D. W.; Schantz, J. T.; Woodruff, M. A.; Teohm, S. H. Evaluation of Polycaprolactone Scaffold Degradation for 6 Months *in vitro* and *in vivo*. *J. Biomed. Mater. Res., Part A* **2009**, *90A*, 906−919.
(35) Lu, Q.; Zhang, B.; Li, M. Z.; Zuo, B. Q.; Kaplan, D. L.; Huang, Y. L.; Zhu, H. S. Degradation Mechanism and Control of Silk Fibroin. *Biomacromolecules* **2011**, *12*, 1080−1086.
(36) He, W.; Yong, T.; Teo, W. E.; Ma, Z. W.; Ramakrishna, S. Fabrication and Endothelialization of Collagen-blended Biodegradable Polymer Nanofibers: Potential Vascular Graft for Blood Vessel Tissue Engineering. *Tissue Eng.* **2005**, *11*, 1574−1588.
(37) Lin, C. H.; Su, J. M.; Hsu, S. H. Evaluation of type II Collagen Scaffolds Reinforced by Poly (ε-caprolactone) as Tissue-Engineered Trachea. *Tissue Eng., Part C* **2008**, *14*, 69−77.
(38) Singh, S.; Wu, B. M.; Dunn, J. C. Delivery of VEGF using Collagen-coated Polycaprolactone Scaffolds Stimulates Angiogenesis. *J. Biomed. Mater. Res., Part A* **2012**, *100*, 720−727.
(39) Timpl, R.; Rohde, H.; Robey, P. G.; Rennard, S. I.; Foidart, J. M.; Martin, G. R. Laminin−a Glycoprotein from Basement Membranes. *J. Biol. Chem.* **1979**, *254*, 9933−9937.
(40) Doran, T. I.; Vidrich, A.; Sun, T. Intrinsic and Extrinsic Regulation of the Differentiation of Skin, Corneal and Esophageal Epithelial Cells. *Cell* **1980**, *22*, 17−25.
(41) Dale, B. A.; Salonen, J.; Jones, A. H. New Approaches and Concepts in the Study of Differentiation of Oral Epithelia. *Crit. Rev. Oral. Biol. Med.* **1990**, *1*, 167−190.
(42) David, A. J.; Paul, J. B.; Darrin, D. B. Culture of Human Keratinocytes in Defined Serum-free Medium. *FOCUS* **1997**, *19*, 2−5.